A new model for predicting of stresses on the compound extrusion container

YUANXIN LUO, YIKUN XIONG, YONGQING WANG, LING MA
The State Key Lab of Mechanical Transmission
Chongqing University
Rm. 320, No. 7 Teaching Building, No.174, Shapingba, 400030, Chongqing
PEOPLE'S REPUBLIC CHINA
yxluo@cqu.edu.cn

Abstract: - The extrusion process is widely used for forming aluminum and titanium alloy parts or products. A material is fed into the extrusion container for pushing through a die to create parts with a fixed cross-sectional profile. The extrusion container is one of the most key components that supports extremely high pressure (>700MPa) in the extrusion process. Therefore, the compound extrusion container is designed for reduce the peak of stresses to increase its reliability. The stresses distribution is largely depended on the interferences and layer thicknesses. In this paper, a new analytical model based on Direction Displacement Method (DDM) is proposed for predicting the stress distribution on the multi-layer container. The stresses distribution on the container after assembly and normal working are computed by using this model. Four cases are studied to verify the fidelity of the proposed model. Finally, discussions and concluding remarks are also given.

Key-Words: - Extrusion process, Extrusion container, Direction Displacement Model (DDM), Finite Element Method (FEM)

1 Introduction

The extrusion process is used most frequently to form aluminum alloy parts or products. A material is fed into the extrusion container for pushing through a die to create objects of a fixed cross-sectional profile. There are two advantages of extrusion process compare to other manufacturing processes are its ability to create complex cross-sections and work with materials which are brittle. It also forms finished parts with good surface (Erik *et. al*, 2000). A typical extrusion press machine is shown in Fig. 1, and the machine consists of main frame, main cylinder, moving cross head, extrusion container and a die set. In general, the extrusion process can be divided into 5 steps: 1) a die set is moved closed to the front platen. 2) Four cylinders push the extrusion container against the die. 3) A billet is fed into the extrusion container. 4) The main ram push the billet flowing though the die, and 5) the container and main ram move to its initial position, and the main shear cut the tailing.

It can be seen that the extrusion container is one of the most key components which exhibit a complex strain-time pattern under a variety of cyclic loading conditions (Mitter *et. al*, 1997). The contact pressure between the workpiece and inner surface the container is ranged from 30MPa to 500 MPa (Bauser *et. al*, 2006). Jo *et. al* (2006) and Mori *et.al* (2002) were studied the inner pressure by numerical method and experiments, respectively. It was also reported that the contact pressure will be even higher than 700MPa for steel. Yoneyama (1999) presented a new sensor to test the contact pressure of layers during extrusion process, which can provide a support to analytical results. Maximum stress always appears on the inner face of single-layer extrusion container. It can be decreased by the peak stress by the usage of the compound container with multi-layer (Mitter *et. al*, 1997). Compare to the transitional single layer container, it can endure higher pressure and it has been widely used in the industry.

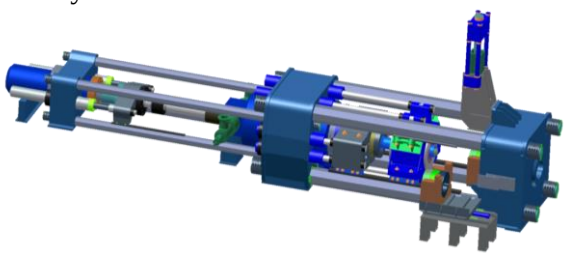

Fig.1: The extrusion press machine and tools

As mentioned above, the extrusion container is in the situation of high temperature and high loads that always interchanged during extrusion, and it is the main reason caused failure. Therefore, it is significant to study the stress distribution on the

container. It has been reported that some effects on has been put on this topic. Krumphals et.al (2011) used FEM to simulate the extrusion process for predicting the temperature and stress evolution in the container, coupled with constitutive equations as well as lifetime consumption models in order to calculate both the inelastic strains and the tools lifetime for optimization of the extrusion process and choosing the right hot work tool steels. They simulated the process by 2D model in Deform and focus on the material life evolution. Pedersen (2000) proposed a model to predict the stresses; however, it's not so efficient to calculate the compound container that consists of multi-layers. Viscoplastic constitutive models were developed in the past to take into account the inelastic behavior of the material during creep–fatigue loads. However, these researches have not considered the residual stress due to shrift fitting assembly process that will be largely impact the stress evolution of the container. Although the numerical studies can be used to predict the stress evolution, it is necessary find the theoretical model that can be used to optimize the design parameters as well as the fitting process.

In this paper, a new method based on elasticity to calculate the contact pressure during extrusion process include the interference fit step and extruding step. It will lead the theoretical foundation for predicting the stresses evolution of the container. Rest of the paper is organized as follows. Section 2 presents the new method Direction Displacement Model (DDM). A comparison study is conducted in in section 3 for demonstration of the effectiveness DDM. Section 4 is the discussions and Section 5 is the conclusion remarks.

2 Direction displacement model for predicting the stresses

The inner pressure of the container is resulted by the plastic deformation of the pallets in the extrusion process. To model the loading and stress on container, following assumptions are made:

1) The dimension tolerance of the each layer is ideally coincided with design parameters.
2) The inner pressure is assumed to be in hydrostatic pressure, and therefore, the pressure applied on the inner surface is the homogeneous distribution.
3) The container is axisymmetric, and the cooling channel and the key slot are neglected in this theoretical study.
4) None force along axial direction.

2.1 Model of single layer container

Based on the assumptions mentioned above, the extrusion container can be simplified into 2-D planar stress state. It can be modeled in a polar coordinator system, and in which there will be none shearing stress. Fig. 2 illustrated a single layer container, and the normal stress and tangential stress can be governed by Eq. (1).

$$\frac{d\sigma_r}{dr}+\frac{\sigma_r-\sigma_t}{r}=0 \tag{1}$$

where, r is within the range of r_i and r_e, σ_r is the radial stress, σ_t is the tangential stress. The relationship between stresses and strains can be expressed as follow:

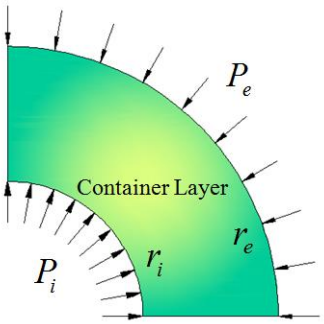

Fig.2: Illustration of single layer container

$$\begin{cases}\sigma_r=\dfrac{E}{1-\mu^2}(\varepsilon_r+\mu\varepsilon_t)\\ \sigma_t=\dfrac{E}{1-\mu^2}(\varepsilon_t+\mu\varepsilon_r)\end{cases} \tag{2}$$

where, E represents the elasticity modulus, μ is the Poisson's ratio, ε_r stands for radial strain and ε_t is the tangential strain. By combination of Eq. (1) and (2), we can get:

$$\frac{E}{1-\mu^2}[\frac{d\varepsilon_r}{dr}+\mu\frac{d\varepsilon_t}{dr}+(1-\mu)(\frac{\varepsilon_r-\varepsilon_t}{r})]=0 \tag{3}$$

The displacement of along radial direction, u, can be expressed by:

$$u=\frac{1}{E(r_e^2-r_i^2)}\cdot [(P_i r_i^2-P_e r_e^2)(1-\mu)r-r_i^2 b^2(P_e-P_i)(1+\mu)\frac{1}{r}], \quad u\in[r_i,r_e] \tag{4}$$

where, r_i and r_e are the inner radius and outer radius, respectively. P_i and P_e are the inner pressure and outer pressure applied on the contact surface.

Assumed that the container is without the inner pressure P_i or outer pressure P_e, Eq. (4) can be rewritten as follow:

$$P_e = 0,\ u = \frac{P_i r_i^2}{E(r_e^2 - r_i^2)}[(1-\mu)r + (1+\mu)\frac{r_i^2}{r}] \quad (5)$$

$$P_i = 0, u = -\frac{P_e r_e^2}{E(r_e^2 - r_i^2)}[(1-\mu)r + (1+\mu)\frac{r_i^2}{r}] \quad (6)$$

2.2 Model of Compound Container

As mentioned previously, the single layer container is not strong enough for modern extrusion industry. The compound container is then proposed with multi-layer by using interference fitting method. In the assembling process, the initial inner radius of outer of each layer is given, and the radiuses will be slightly changed due to the interference fitting, or external loading. In general, there are two cases should be considered that are applied interference fitting and external loading. We will use DDM for computing the amount of radius changing. Then the Lame equations are used for calculating the stresses.

As showing Figure 3, $\delta_{i-1,i}$ is defined as the amount of interfere of Layer i (i=2,3,...,n) and Layer i-1. Based on the physical meaning of the definition that can be calculated by subtracting initial outer radius $r_{i-1,out}$ of Layer i-1 and initial inner radius $r_{i,in}$ of Layer i, it can be expressed by:

$$\delta_{i-1,i} = \left| r_{i-1,out} - r_{i,in} \right| \quad (7)$$

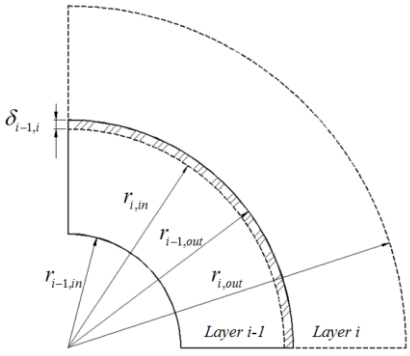

Fig.3: Illustration of interference fitting of multi-layer

As illustrated in Fig. 4, $r_{1,in}$ initial inner radius of Layer 1, and $r_{n,out}$ initial outer radius of the outer layer. r_i (i=2,3,...,n-1) is the radius of the ith contact surface. $\delta_{i-1,i}$ is the interference and $P'_{0,1}$ is the external load on the inner radius of Layer 1. It is obviously that the loading of Layer 1 and Layer n are different from the other layers.

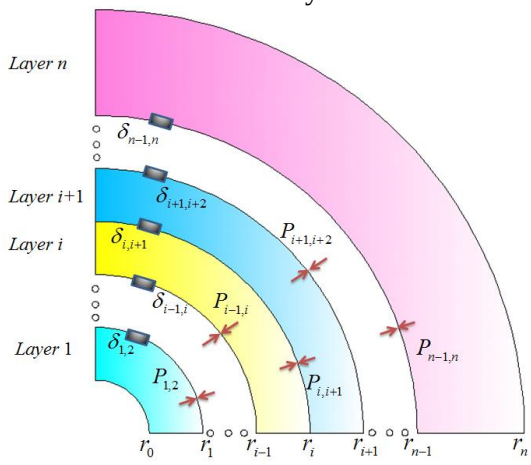

(a)

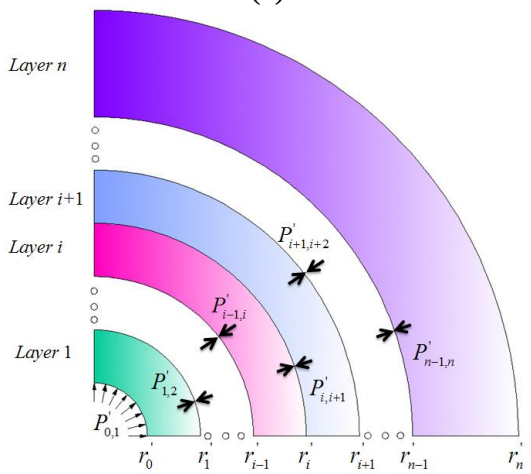

(b)

Fig.4: Illustration of loading on a multi-layer container. (a) With interference fitting; (b) With external loading.

2.2.1 Interference fitting process

As shown in Figure 4 (a), it can be easier found that the formulas form the single layer model can be used for describing the compound container, that is: Eq. (5) can be used for expressing the inner layer; Eq. (6) can be used for describing the outer layer, while Eq. (5) is for the others. There can be rewritten in Eq. (8), Eq. (9) and Eq. (10), respectively.

$$\begin{cases} r_0 - r_{1,in} = \dfrac{2P_{1,2} r_{1,in} r_{1,out}^2}{E(r_{1,out}^2 - r_{1,in}^2)} \\ r_1 - r_{1,out} = \dfrac{P_{1,2} r_{1,out}}{E} \times \left(\dfrac{r_{1,out}^2 + r_{1,in}^2}{r_{1,out}^2 - r_{1,in}^2} - \mu \right) \end{cases} \quad (8)$$

$$\begin{cases} r_{n-1} - r_{n,in} = \dfrac{P_{n-1,n} r_{n,in}}{E} \times \left(\dfrac{r_{n,out}^2 + r_{n,in}^2}{r_{n,out}^2 - r_{n,in}^2} + \mu \right) \\ r_n - r_{n,out} = \dfrac{2P_{n-1,n} r_{n,out} r_{n,in}^2}{E(r_{n,out}^2 - r_{n,in}^2)} \end{cases} \quad (9)$$

$$\begin{cases} r_{i-1} - r_{i,in} = \dfrac{1}{E(r_{i,out}^2 - r_{i,in}^2)} [(P_{i-1,i} r_{i,in}^2 - P_{i,i+1} r_{i,out}^2)(1-\mu) r_{i,in} \\ -r_{i,in}^2 r_{i,out}^2 (P_{i,i+1} - P_{i-1,i})(1+\mu) \dfrac{1}{r_{i,in}}] \\ r_i - r_{i,out} = \dfrac{1}{E(r_{i,out}^2 - r_{i,in}^2)} [(P_{i-1,i} r_{i,in}^2 - P_{i,i+1} r_{i,out}^2)(1-\mu) r_{i,out} \\ -r_{i,in}^2 r_{i,out}^2 (P_{i,i+1} - P_{i-1,i})(1+\mu) \dfrac{1}{r_{i,out}}] \\ i = 2,3,...,n \end{cases} \quad (10)$$

By solving the sets of equations, the contact pressure, Pi-1,i , on each contact surface after interference fitting for the given initial radius of $r_{i,in}$ (i=2,3,...,n) and $r_{i,out}$ (i=1,2,...,n-1).

2.2.2 Applied external loading

This case is similar to the previous one, as illustrated in Figure 4(b). It can be derived from Eq. (4), Eq. (5) and Eq. (6) for describing the relationships as shown in Eq. (11) and Eq. (12).

$$\begin{cases} r_{n-1}^{'} - r_{n,in} = \dfrac{P_{n-1,n}^{'} r_{n,in}}{E} \times \left(\dfrac{r_{n,out}^2 + r_{n,in}^2}{r_{n,out}^2 - r_{n,in}^2} + \mu \right) \\ r_n^{'} - r_{n,out} = \dfrac{2P_{n-1,n}^{'} r_{n,out} r_{n,in}^2}{E(r_{n,out}^2 - r_{n,in}^2)} \end{cases} \quad (11)$$

$$\begin{cases} r_0^{'} - r_{1,in} = \dfrac{1}{E(r_{1,out}^2 - r_{1,in}^2)} [(P_{0,1}^{'} r_{1,in}^2 - P_{1,2}^{'} r_{1,out}^2)(1-\mu) r_{1,in} \\ -r_{1,in}^2 r_{1,out}^2 (P_{1,2}^{'} - P_{0,1}^{'})(1+\mu) \dfrac{1}{r_{1,in}}] \\ r_i^{'} - r_{i,out} = \dfrac{1}{E(r_{i,out}^2 - r_{i,in}^2)} [(P_{i-1,i}^{'} r_{i,in}^2 - P_{i,i+1}^{'} r_{i,out}^2)(1-\mu) r_{i,in} \\ -r_{i,in}^2 r_{i,out}^2 (P_{i,i+1}^{'} - P_{i-1,i}^{'})(1+\mu) \dfrac{1}{r_{i,in}}] \\ r_i^{'} - r_{i+1,in} = \dfrac{1}{E(r_{i,out}^2 - r_{i,in}^2)} [(P_{i-1,i}^{'} r_{i,in}^2 - P_{i,i+1}^{'} r_{i,out}^2)(1-\mu) r_{i,out} \\ -r_{i,in}^2 r_{i,out}^2 (P_{i,i+1}^{'} - P_{i-1,i}^{'})(1+\mu) \dfrac{1}{r_{i,out}}] \\ i = 1,2,...,n-1 \end{cases} \quad (12)$$

where, $r_n^{'}$ ($i=1,3,...,n$) represents the radius of contact surfaces with applied loading.

By solving the sets of equations, the contact pressure, $P_{i-1,i}^{'}$ (i=1,3,...,n), on each contact surface after interference fitting for the given initial radius of $r_{i,in}$ (i=2,3,...,n) and $r_{i,out}$ (i=1,2,...,n-1). Also, the radius $r_n^{'}$ are obtained as the meantime.

2.2.3 Stress computation

With given inner pressure, outer pressure, initial and final radius, the Lame equations (Laue and Stenger, 1981), as given in Eq. (13), is available for calculating the stress distribution of each layer along radial direction. Then, the Mises stress can be obtained by using Eq. (14):

$$\begin{cases} \sigma_r = \dfrac{p_i r_i^2 - p_e r_e^2}{r_e^2 - r_i^2} + \dfrac{r_i^2 r_e^2 (p_i - p_e)}{r_e^2 - r_i^2} \dfrac{1}{r^2} \\ \sigma_t = \dfrac{p_i r_i^2 - p_e r_e^2}{r_e^2 - r_i^2} - \dfrac{r_i^2 r_e^2 (p_i - p_e)}{r_e^2 - r_i^2} \dfrac{1}{r^2} \end{cases} \quad (13)$$

$$\sigma_{Mises} = \left[\frac{1}{2} \left[(\sigma_r - \sigma_t)^2 + \sigma_r^2 + \sigma_t^2 \right] \right]^{\frac{1}{2}} \quad (14)$$

3 A comparative study of DDM and FEM

Four design extrusion container with tri-layers are comparative studied is this comparison. The design parameters are given in *Appendix* Table 1.

3.1 Contact pressure on the contact surfaces

The contact pressure is calculated by the proposed model, as shown in *Appendix* Table. 2. As the container model is simplified to asymmetrical. A 3D FEM model is built by taking a quarter of the container for effective computing, as shown in Fig. 5. Assume that the stresses along axial direction are uniform and small. Also, thermal stress are not been taken into consideration. The property of material is homogeneous and elasticity. The model are simplified and without any small features. The averaged of contact pressure is summarized in *Appendix* Table 3.

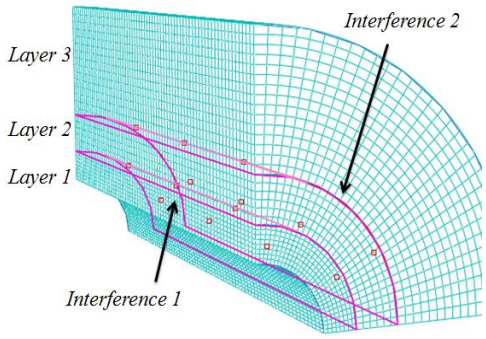

(a)

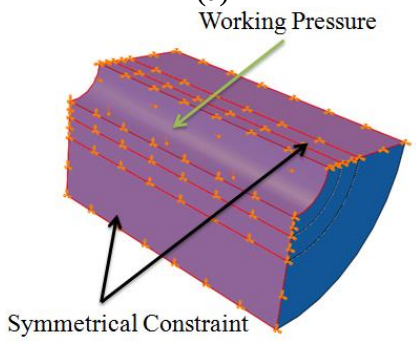

(b)

Fig.5: FEM model of the compound container. (a) FEM mesh; (b) boundary conditions.

From results shown in Table 2 and Table 3, it is can be found of that DDM results are with agree with FEM results with the maximum error of 0.5%. It indicates that the DDM is effective method to calculating the contact pressure.

3.2 Stresses distribution predicting by DDM

By using the DDM, the stress distribution along the radial direction are obtained as shown in Figure 6.

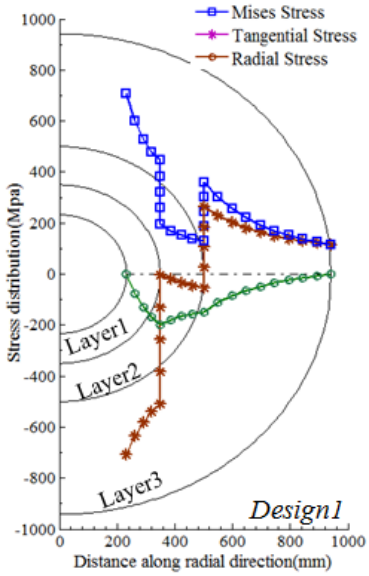

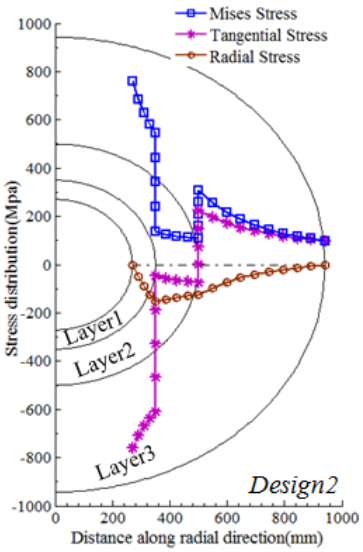

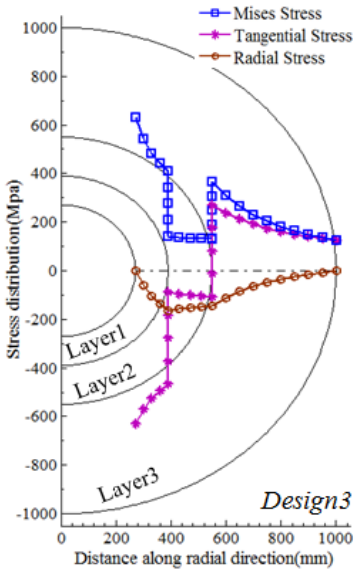

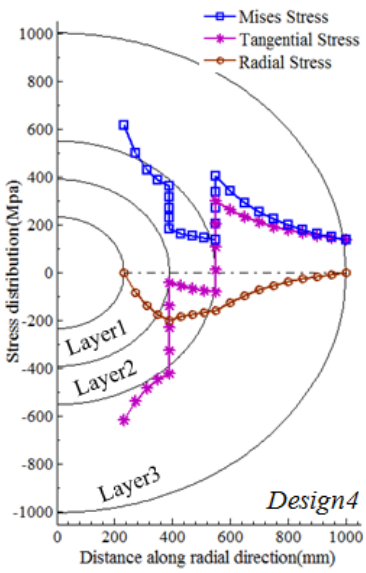

(a)

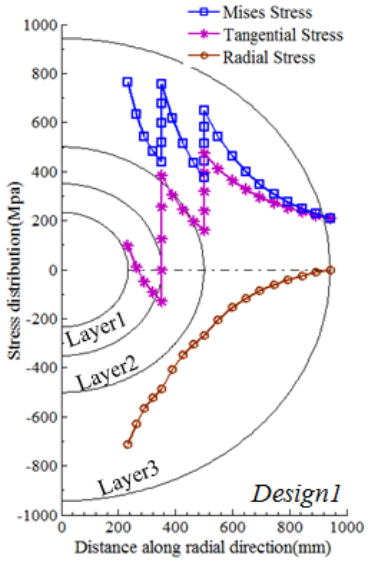

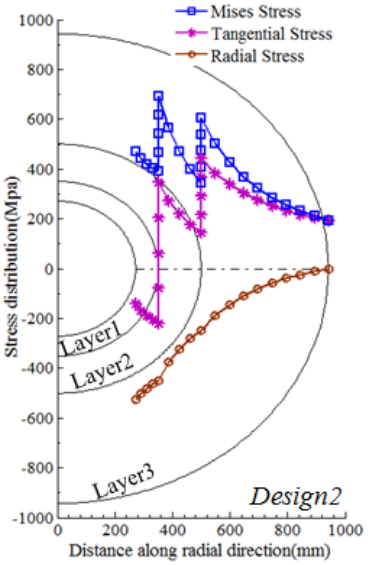

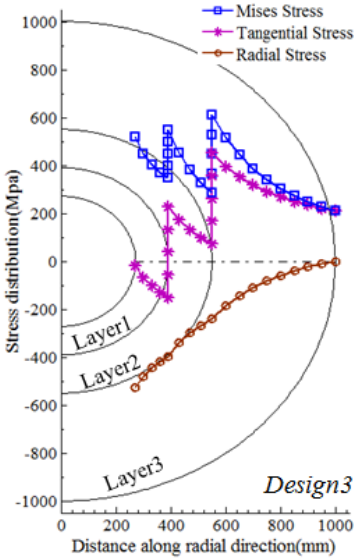

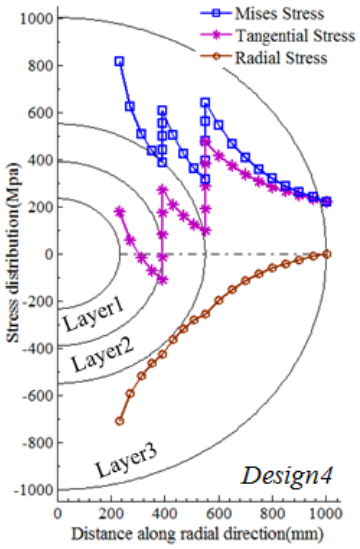

(b)

Fig.6: Stresses distributions by DDM. (a) Case 1; (b) Case 2.

From the results given in Fig. 6, it can be seen that the tangential stresses for the inner layer will be decreased for reducing its thickness. The peak stresses are appeared on the inner surface. However, the max principle stresses will reduced or appear in the other layers when the design parameters are optimized. The stresses on Layer 1 are compressed after assembly and tension during extrusion process. Its safety factor is higher than that of single layer container.

4 Discussions

Some functions, such as heating, cooling, and thermal measuring, etc., are integrated in modern extrusion container that is so called smart container (Benedyk, 2008). On the other hand, the container should be mounted on a container house, and therefore, the key slots are necessary for connecting. So, there are some small structure features, e.g., holes, grooves, are designed to realize these functions. These feathers will change the local stresses distributions and cause stress concentrations. A compound container is shown in Fig.7, and it requires FEM to predict the local stresses.

Using the same parameters as Design 1 mentioned in section 3 and considering the small size feathers, FEM simulation are conducted in Abqus™ and the results are shown in Fig. 8. It can be seem from the results, there are many peak stresses appeared on layers due to the non-uniform

contact surface. However, the average of the contact pressure is approximated to DDM results, and also the distribution of contact press on Layer 3 is similar to DDM result. This is probably because the contact surface is without any changes.

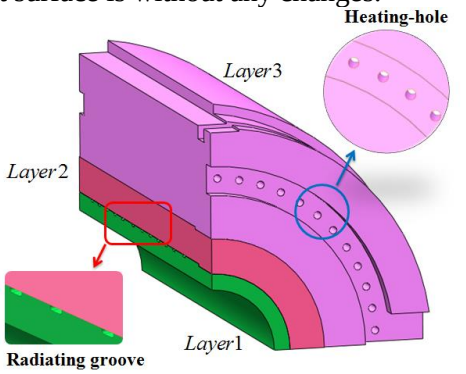

(a)

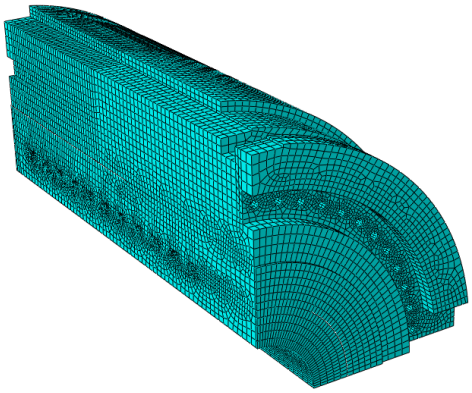

(b)

Fig.7: Compound containers. (a) CAD model; (b) FEM mesh.

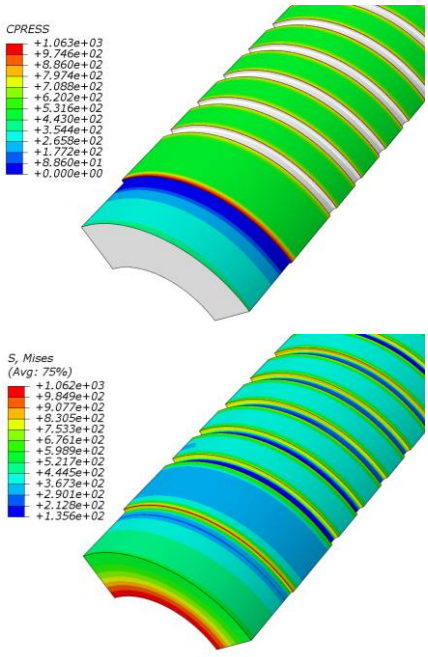

(a)

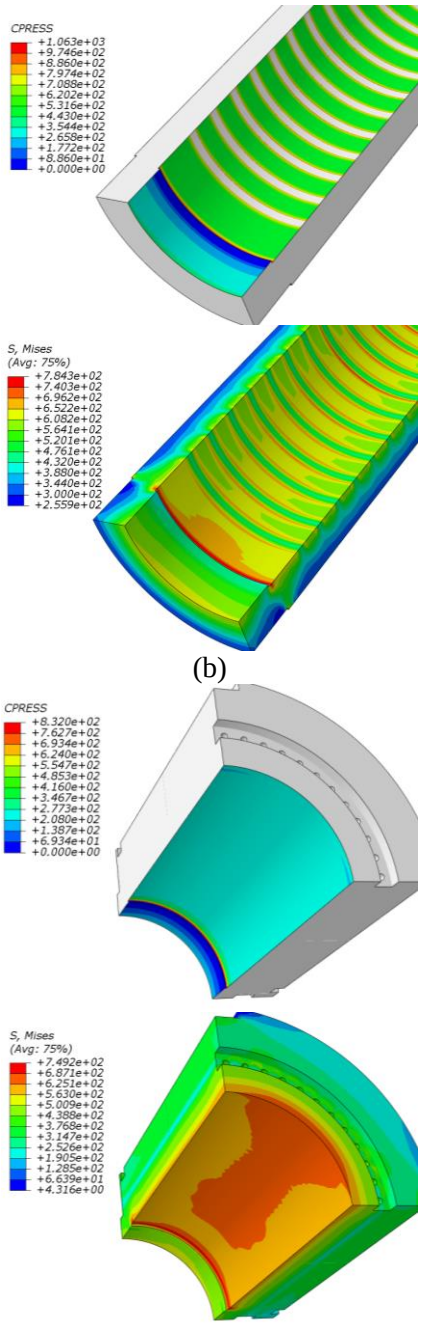

(b)

(c)

Fig.8: CPRESS and Mises stress of extrude container by FEM. (a) Layer 1; (b) Layer 2; (c) Layer 3.

5 Conclusions

This paper presents a new method, so called DDM, based on elasticity for predicting the contact pressure during extrusion process. It can be used to analyze stresses distributions on the container for the shrift fit process and the extrusion process. The concluding remarks are given as follow:

1) By comparing the FEM results and DDM results, it indicates that the proposed DDM

model are well predicted the contact pressure of the compound container after shift fitting and during extrusion.

2) By integrating of DDM and Lame's equation, the stresses can also be calculated, and the stress distributions along the radial direction are obtained.
3) From the stress curves, it can be seen that compound container will significantly decrease the peak stress than that of single layer container. The stresses can be reduced by carefully design of the parameters and tolerance. The DDM model will be the fundamental model for the optimization of container.
4) Finally, some small size feather should be analyzed in FEM that will be more precise for predicting the stress concentrations.

Acknowledgements

This project is supported by National Natural Science Foundation of China (Grant No. 51345013) and National Science and Technology Major Project of the Ministry of Science and Technology of China (Grant No. 2011ZX04016-081).

References:

[1] Erik, O., Franklin, J., Horton, D., Holbrook, L., Henry, R., Machinery's Handbook (26th ed.) (2000), Industrial Press.
[2] Mitter, W., Haberfellner, K., Danzer, R., Stickler, C. Life time prediction of hot work tool steels, HTM - Haerterei-Technische Mitteilungen, Vol. 52 (1997), pp. 253-258.
[3] Bauser, M., Sauer, G., Siegert, K., Extrusion, ASM International, 2006.
[4] Jo, H.H., Lee, S.K., Jung, C.S., Kim, B.M., A non-steady state FE analysis of Al tubes hot extrusion by a porthole die, Journal of Materials Processing Technology, Vol. 173 (2006), pp.223-231.
[5] Mori, T., Takatsuji, N., Matsuki, K., Aida, T., Murotani, K., Uetoko, K., Measurement of pressure distribution on die surface and deformation of extrusion die in hot extrusion of 1050 aluminum rod, Journal of Materials Processing Technology, Vol. 130-131 (2002), pp.421-425.
[6] Yoneyama, T., Development of a new pressure sensor and its application to the measurement of contacting stress in extrusion, Journal of Material Processing Technology, Vol. 95 (1999) , pp.71-77.
[7] Krumphals, F., Wlanis, T., Sievert, R., Wieser, V., Sommitsch, C., Damage analysis of extrusion tools made from the austenitic hot work tool steel Böhler W750, Computational Materials Science, Vol. 50 (2011), pp.1250-1255.
[8] Pedersen, T., Numerical studies of low cycle fatigue in forward extrusion dies, Journal of Materials Processing Technology, Vol.105 (2000), pp. 359-370.
[9] Laue, K., Stenger, H., Extrusion: processes, machinery, tooling (1981), American Society for Metals.
[10] Benedyk, J. C., The Evolution of the Smart Container: Achieving Isothermal Control in Extrusion. Light Metal Age, Vol. 1 (2008), pp.40-44.

Appendix

Table 1 Design parameters of the four cases.

	r_0 / *mm*	$r_1^{'}$ / *mm*	$r_2^{'}$ / *mm*	r_3 / *mm*	$\Delta\delta_{1,2}$ / *mm*	$\Delta\delta_{2,3}$ / *mm*	P_0 / *MPa*
Design 1	233.5	350	500	942	1.7	1.5	712.0
Design 2	271.5	350	500	942	1.88	1.42	526.8
Design 3	271.5	390	550	1000	1.404	1.98	526.8
Design 4	233.5	390	550	1000	1.404	1.98	712.0

Table 2 Contact pressure calculated by using the DDM.

DDM	Case 1/ MPa		Case 2/ MPa	
	@ Inteference1	@ Inteference2	@ Inteference1	@ Inteference2
Design 1	197.42	147.72	487.58	266.27
Design 2	153.07	126.00	449.70	247.22
Design 3	163.06	144.94	396.09	241.45
Design 4	198.94	159.69	427.08	254.29

Table 3 Average contact pressure of FEM

FEM	Case 1/ MPa		Case 2/ MPa	
	@ Inteference1	@ Inteference2	@ Inteference1	@ Inteference2
Design 1	196.91	147.36	487.94	266.19
Design 2	152.15	125.51	450.16	247.20
Design 3	162.57	144.57	396.29	241.24
Design 4	198.68	159.51	426.53	253.75